JOURNAL OF Materials CHEMISTRY

Cation deficient $Cu_{4-x}GeCo_4Sn_{12}S_{32}$ thiospinels: electrochemical behaviour and induced structural modifications

Carlos Pérez Vicente,*[a] José L. Tirado,[a] Christelle Bousquet,[b] Josette Olivier Fourcade[c] and Jean C. Jumas[c]

[a]*Laboratorio de Química Inorgánica, Facultad de Ciencias, Universidad de Córdoba, Avda San Alberto Magno s/n, 14004 Córdoba, Spain. E-mail: iq3pevic@uco.es*
[b]*Laboratoire de Physicochimie de la Matière Condensée (UMR 5617 CNRS), Place Eugène Bataillon, 34095 Montpellier Cedex 5, France*
[c]*Laboratoire des Agrégats Moléculaires et Matériaux Inorganiques (ESA 5072 CNRS), Place Eugène Bataillon, 34095 Montpellier Cedex 5, France*

Received 1st April 1999, Accepted 29th June 1999

Characterization of the structure and electrochemical behaviour of two deficient thiospinels, $Cu_4GeCo_4Sn_{12}S_{32}$ and $Cu_{2.6}GeCo_4Sn_{12}S_{32}$, where the latter was obtained by chemical deintercalation of Cu from the former, has been performed. The structural study shows that tetragonal distortion is present in $Cu_4GeCo_4Sn_{12}S_{32}$, due to the Jahn–Teller effect for low-spin Co^{II}, while this distortion is negligible for $Cu_{2.6}GeCo_4Sn_{12}S_{32}$ with partial oxidation of Co^{II} to Co^{III}.

The electrochemical study of lithium insertion into $Cu_4GeCo_4Sn_{12}S_{32}$ reveals the presence of three well defined voltage steps located at *ca.* 2.15, 1.67 and <1.65 V. The spinel structure is preserved during the first steps of lithium insertion, while a two-phase region is observed for $x \geqslant 6$. The step at 2.15 V can be attributed to the filling of vacancies in tetrahedral sites. When $Cu_{2.6}GeCo_4Sn_{12}S_{32}$ is used as an active cathode material, a new lithium insertion process appears in the first step of the discharge curve, centered at *ca.* 2.24 V, followed by others at 2.13 and <1.8 V, the host framework is also retained during the Li insertion. The new first step may be attributed to Co^{III}–Co^{II} reduction while the second step at 2.13 V is assigned to the filling of tetrahedral vacancies, accompanied by copper extraction. Finally, ^{119}Sn Mössbauer spectroscopy shows that the Sn^{IV}–Sn^{II} reduction takes place at a large depth of discharge.

Introduction

The thoroughly studied AB_2X_4 spinel-type structure can be described as an array of parallel chains of octahedra sharing opposite edges, which run perpendicular and join by edge sharing to chains in adjacent levels. Irrespective of the possible presence of ions in tetrahedral coordination, the array of octahedra provides a rigid network extending in three dimensions which defines a notably large number of empty interstitial sites possessing both tetrahedral and octahedral coordination. The stability of such an array is clearly shown by the fact that some B_2X_4 solids have been isolated, such as λ-MnO_2.[1] In addition, a vast number of cation-deficient solids have been reported. Particularly among chalcogenides, numerous examples are found which include binary (tin–indium thiospinels),[2] ternary ($Cu_xTi_2S_4$),[3] quaternary ($Cu_2MSn_3S_8$, M = Mn, Fe, Co, Ni)[4] and five-element ($Cu_{3.31}GeFe_4Sn_{12}S_{32}$)[5] phase compositions. For the latter compound, the extended formula can be written (including the Wyckoff symbols of the equivalent sites occupied by cations in the $Fd\bar{3}m$ space group), as: $(Cu_{3.31}Ge\square_{3.69})_{8a}[Fe_4Sn_{12}]_{16d}S_{32}$. The solid can be prepared from the pure elements and can be regarded as the result of a topotactic substitution of Cu^+ by Ge^{4+} in a 4:1 ratio in $Cu_2FeSn_3S_8$. The same synthetic procedure applied to the cobalt-derivative which is reported here allowed the preparation of a solid with less marked cation deficiency and stoichiometry, $Cu_4GeCo_4Sn_{12}S_{32}$.

On the other hand, many of these spinel chalcogenides have proven to be interesting host lattices for lithium intercalation reactions. However, their application as high-performance intercalation electrodes is commonly restricted by several undesirable factors such as repulsions between the incoming lithium ions and cations in 8a sites, and possible cation redistribution induced by changes in the oxidation states of the transition metal ions. These limitations can be controlled in part by generating cation vacancies in the tetrahedral coordination sites. This can be achieved during the synthesis procedure as described above. Alternatively, extraction of some of the ions in tetrahedral sites prior to the use of the lithium intercalation electrode can be achieved by chemical procedures, such as oxidation under mild conditions (*e.g.* by the use of I_2–CH_3CN solutions),[3,4] and leads to a better cycling behaviour of the resulting solids in lithium-anode and lithium-ion cells.[6,7] This procedure is applied here to the $Cu_4GeCo_4Sn_{12}S_{32}$ system and the electrochemical performance of the material before and after extraction is evaluated.

Experimental

To obtain the compound $Cu_4GeCo_4Sn_{12}S_{32}$, a stoichiometric mixture of the pure elements was sealed under vacuum in a quartz tube. The mixture was heated to 250 °C, at a constant rate of 50 °C h^{-1} and maintained at this temperature for 48 h, then the temperature was increased to 680 °C for a week and finally slowly cooled to room temperature. The copper extraction was carried out by treating the compound with a 0.1 mol dm^{-3} solution of I_2 in CH_3CN, as the oxidation reagent.[3,4]

Electrochemical lithium insertion was carried out in two-electrode cells. The cathode was a pellet of the active compound of diameter 7 mm and mass *ca.* 25 mg. The anode was a lithium disk and the electrolyte was a 1 mol dm^{-3} solution of $LiClO_4$ in propylene carbonate supported in a

glass–paper disk (Whatman Glass Microfibre). The discharge curves were obtained by using a MacPile multichannel microprocessor-controlled system. An initial relaxation was allowed until $\Delta V/\Delta t$ was <1 mV h^{-1}. The current density used for the discharge was *ca.* 50 μA cm^{-2} ($\approx$1 Li mol^{-1} in 12 h). The different lithiated samples were obtained by interrupting the discharge at the desired composition, on the assumption that no current was due to side reactions.

X-Ray diffraction patterns (XRD) were recorded on a Siemens D500 diffractometer, using Cu-Kα radiation. For lithium inserted solids, the electrodes prepared by interrupting discharge experiments were allowed to reach equilibrium for 8 weeks prior to XRD and Mössbauer studies. To avoid the oxidation of the lithiated products, the electrodes were stored in a glove box (M. Braun), and were covered with a thin plastic film during the recording of their XRD patterns. Rietveld analyses of the XRD patterns of the different samples, when possible, was carried out with the aid of the computer program DBWS-9411.[8]

^{119}Sn Mössbauer spectra were recorded at room temperature in the constant acceleration mode on an ELSCINT-AME40 spectrometer. The γ-ray source was ^{119m}Sn in a matrix of $BaSnO_3$. The velocity scale was calibrated with the magnetic sextet spectrum of a high purity iron foil absorber, using ^{57}Co(Rh) as the source. The recorded spectra were fitted to lorentzian profiles by a least squares method.[9] The origin of the isomer shift was determined from the center of the $BaSnO_3$ spectrum recorded at room temperature.

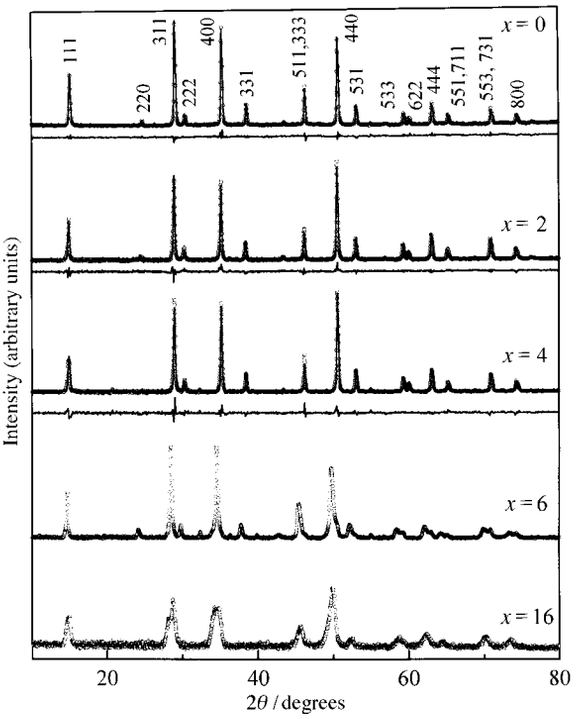

Fig. 1 X-Ray diffraction patterns and Rietveld refinement of $Li_xCu_4GeCo_4Sn_{12}S_{32}$ at selected x values.

Results and discussion

The direct synthesis procedure used here leads to a powdered solid with stoichiometry $Cu_4GeCo_4Sn_{12}S_{32}$. The X-ray diffraction pattern of this solid can be indexed according to the cubic $Fd\bar{3}m$ space group (Fig. 1). A Rietveld refinement of the structural parameters was carried out by assuming the following atom distribution: $(Cu_4Ge)_{8a}(Co_4Sn_{12})_{16d}(S_{32})_{32e}$ with random distribution of cations in 8a and 16d sites. The results collected in Table 1 reveal a Bragg R factor of $<5\%$.

The ^{119}Sn Mössbauer spectrum of the $Cu_4GeCo_4Sn_{12}S_{32}$ powder is shown in Fig. 2. The presence of a single quadrupole-split signal with its centroid at 1.173(6) mm s^{-1} is the only feature in this spectrum (Table 2). The isomer shift values are consistent with formal Sn^{IV} oxidation state in octahedral coordination. This unequivocally involves the Cu^{I} and Co^{II} oxidation states, as found in other related systems.[4] On the other hand, the value of the quadrupolar splitting parameter (QS) in Table 2 is indicative of a slight deviation from cubic symmetry for the Sn^{IV} species. Its origin will be discussed below.

The pristine spinel sulfide was used as the active cathode material in lithium anode cells. Fig. 3 shows three alternative representations of the discharge profile. The V *vs.* x (in $Li_xCu_4GeCo_4Sn_{12}S_{32}$) plot [Fig. 3(a)] reveals three well defined voltage steps B, C and D with plateaux located at *ca.* 2.15, 1.67 and <1.65 V, where B and C are separated by a steep decrease in voltage at *ca.* 3.2 F mol^{-1}. These effects lead to two well separated reduction bands in the reciprocal derivative plot $-dx/dV$ *vs.* x [Fig. 3(b)] and the corresponding peaks at particular voltages in Fig. 3(c), while a degree of overlap takes place between the C and D processes. From these plots, it is of note that the compositional upper limit for the first step matches fairly well with the number of lithium atoms per unit cell formula required to completely fill the 8a sites of the cubic spinel structure. The second and third steps could then involve the progressive occupancy of the remaining pseudo octahedral 16c or tetrahedral 8b sites. Further information about these

Table 1 Refined structural parameters and reliability factors for $Cu_4GeCo_4Sn_{12}S_{32}$ and $Cu_{2.6}GeCo_4Sn_{12}S_{32}$ at different depths of discharge, expressed in terms of F mol^{-1} of active material[a]

				Reliability factors (%)			
F mol^{-1}	a/Å	x in 32e(x,x,x)	Cu in 8a (refined)	R_p	R_{wp}	S	R_{Bragg}
$Li_xCu_4GeCo_4Sn_{12}S_{32}$							
0	10.105(1)	0.2503(2)	3.98(1)	7.08	9.40	1.67	4.82
2	10.199(2)	0.2497(2)	3.9(1)	8.50	11.02	1.99	6.17
4	10.239(2)	0.2503(2)	3.8(1)	7.27	9.44	2.10	5.45
$Li_xCu_{2.6}GeCo_4Sn_{12}S_{32}$							
0	10.165(1)	0.2536(3)	2.58(9)	7.76	10.67	1.62	3.21
4	10.172(1)	0.2543(3)	2.06(8)	8.34	12.64	2.08	2.94
6	10.178(1)	0.2544(3)	2.1(1)	10.58	15.31	2.85	4.09

$Cu_4GeCo_4Sn_{12}S_{32}$ (refined according to $I4_1/amd$)						Reliability factors (%)			
F mol^{-1}	a_T/Å	c_T/Å	y	z	Cu in 4a (refined)	R_p	R_{wp}	S	R_{Bragg}
0	7.157(1)	10.109(2)	0.008(1)	0.242(1)	3.8(1)	6.80	9.09	1.61	3.40

[a]For space group $Fd\bar{3}m$, atoms are located in sites 8a (Cu and Ge), 16d (Sn and Co) and 32e (S). For $I4_1/amd$, the sites are 4a, 8d and 16h, respectively.

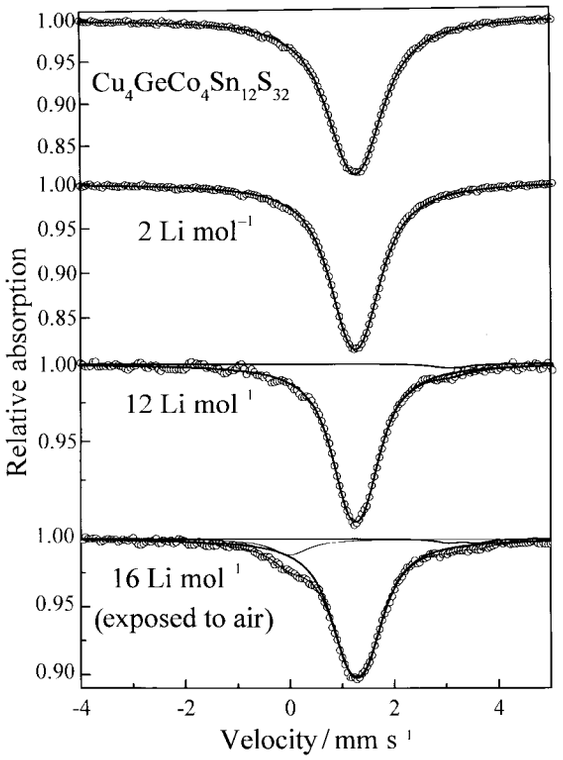

Fig. 2 Experimental and refined ^{119}Sn Mössbauer spectra of $Li_xCu_4GeCo_4Sn_{12}S_{32}$ at selected x values.

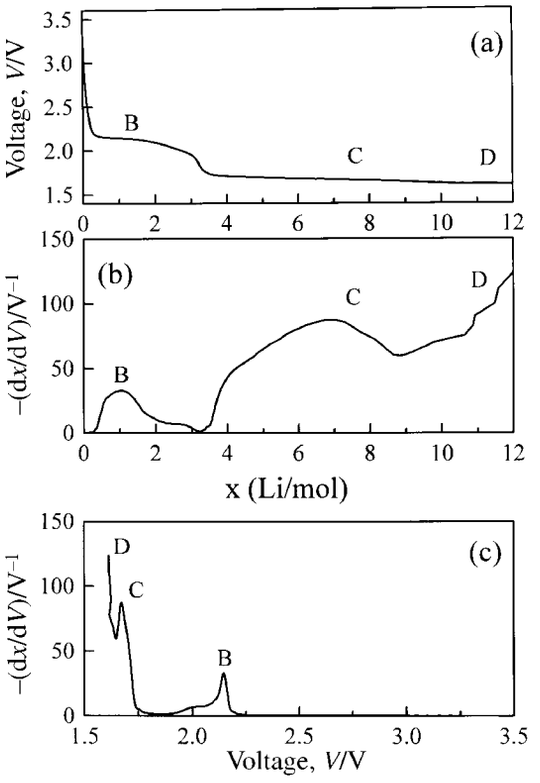

Fig. 3 Discharge curve of the cell $Li|LiClO_4$–PC$|Cu_4GeCo_4Sn_{12}S_{32}$: voltage V *vs.* x (a), $-dx/dV$ *vs.* x (b) and $-dx/dV$ *vs.* V (c).

possibilities was obtained from XRD and Mössbauer spectroscopy data.

Fig. 1 also shows the XRD patterns of the electrode pellets obtained by interrupting the discharge experiments at selected values of the composition parameter x. These data unambiguously show that the spinel structure of this compound is preserved during the first steps of discharge. Nevertheless, a distinct loss of crystallinity is observed above $x=6$, as evidenced by the enhanced line broadening. Moreover, a close inspection of the XRD patterns reveals the presence of shoulders in the line profiles, which suggests that for $x \geqslant 6$ there is a mixture of two phases, as expected from the lower voltage plateaus present in the discharge curves (Fig. 3). These phenomena limit the possible application of the Rietveld refinement procedure to the data obtained above $x=4$. Nevertheless, cubic unit cell parameters were obtained by the least-squares procedure for all compositions, by selecting the higher intensity lines of the two-phase products ($x \geqslant 6$). These results are shown in Fig. 4(a) and evidence a significant increase in lattice constant a from the pristine solid to $x=6$. Further insertion leads to values which differ by less than the experimental error. This two-step behaviour is in good agreement with the electrochemical behaviour discussed above and with the presence of a two-phase system for $x \geqslant 6$ Li mol^{-1}. From these results, the occurrence of the two phases can not be ascribed to a non-homogenous distribution of lithium in the particles of the electrode material, as this should affect the whole range of compositions, while multiple XRD lines were not detected below $x=6$.

Alternatively, a possible spinel to rock-salt structural conversion gives a better explanation of the observed behaviour. Thus, after occupying the vacant tetrahedral 8a sites, additional Li could occupy the 16c sites, with an associated cation migration from 8a to 16c sites, thereby minimizing repulsion effects, as previously described in related spinel oxides and chalcogenides, such as Fe_3O_4,[10] $ZnCo_2O_4$,[11] $Li_{4+x}Ti_5O_{12}$,[12] $CuZr_2S_4$[13] and $Cu_{3.31}GeFe_4Sn_{12}S_{32}$.[5]

Further insight on the mechanism of insertion was obtained by Rietveld analysis of XRD patterns of samples with $x=2$ and 4. The calculated and difference profiles obtained by Rietveld refinement for these compositions are shown in Fig. 1, while Table 1 lists values of the refined parameters. These results show that the occupancy of 8a sites by copper atoms decreases slightly from 0 to 4 F mol^{-1}. However, as the observed change falls within the standard deviation range, copper extraction cannot be unambiguously confirmed during the first steps of lithium insertion. This may not be the case at deeper discharges for which the Rietveld refinement could not be carried out. Copper extraction has been observed in other related systems, where it was unambiguously shown that copper extraction from the spinel structure takes place during lithium insertion.[5,13]

The ^{119}Sn Mössbauer spectra of the different lithiated samples show only one quadrupole-split signal for $x \leqslant 10$. At $x=12$, the presence of Sn^{II} was revealed by a low-intensity shoulder at *ca.* 3 mm s^{-1}, as shown in Fig. 2. Further lithium insertion is accompanied by an increase in the amount of Sn^{II}. For $x=16$, a third signal at *ca.* 0 mm s^{-1} is clearly evident in

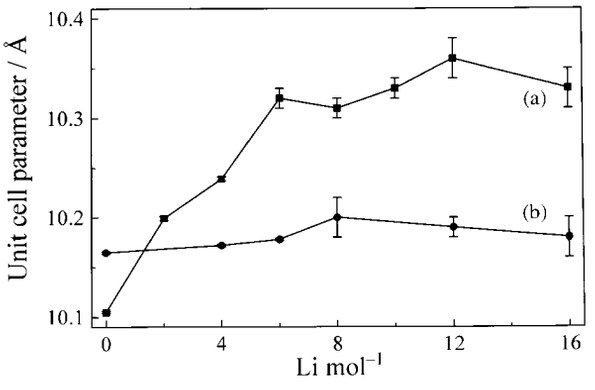

Fig. 4 Evolution of the unit cell parameter of $Cu_4GeCo_4Sn_{12}S_{32}$ (a) and $Cu_{2.6}GeCo_4Sn_{12}S_{32}$ (b) as a function of the depth of discharge.

the spectrum, which can be attributed to the oxidation of Sn^{II} to SnO_2 by unavoidable contact with air (Fig. 2). A similar phenomenon was described during a study of the product of Cp_2Co intercalation into SnS_2, where the reaction Sn^{II} to SnO_2 was shown to be semiquantitative.[14] From these results, it can be inferred that step D in the discharge curve of Fig. 3 is due to the Sn^{IV}–Sn^{II} reduction reaction.

The pristine $Cu_4GeCo_4Sn_{12}S_{32}$ powders were treated with I_2–CH_3CN solution, where the reaction shown in eqn. (1) was expected

$$Cu_4GeCo_4Sn_{12}S_{32} + (y/2)I_2 \rightarrow Cu_{4-y}GeCo_4Sn_{12}S_{32} + yCuI \quad (1)$$

The X-ray diffraction pattern of the product of the above chemical reaction agrees well with the Cu extraction process affecting all particles homogeneously, as single lines were present in the XRD patterns that could be indexed according to a single phase belonging to the cubic $Fd\bar{3}m$ space group (Fig. 5). The observed increase in the relative intensity of the (111) reflection implies a decrease in the average atomic scattering factor of ions in tetrahedral 8a sites. The quantitative evaluation of these changes results in the Rietveld refined structural parameters which are included in Table 1. The Cu occupancy of the 8a site of 2.58(9), indicates that *ca.* 1.4 Cu have been extracted during the treatment with I_2–CH_3CN. In consequence, the number of vacancies in the 8a sites increases from the initial value of 3.0 to *ca.* 4.4.

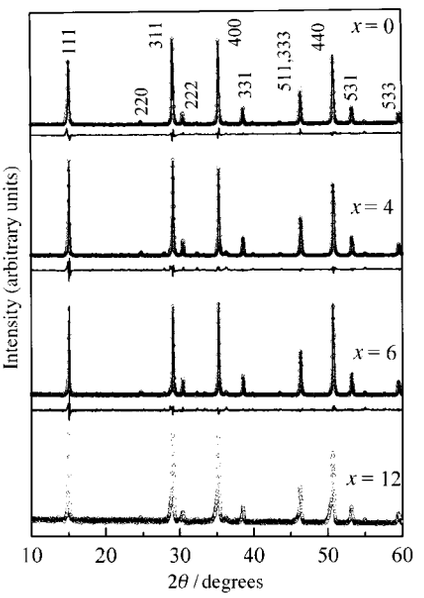

Fig. 5 X-Ray diffraction patterns and Rietveld refinement of $Li_xCu_{2.6}GeCo_4Sn_{12}S_{32}$ at selected x values.

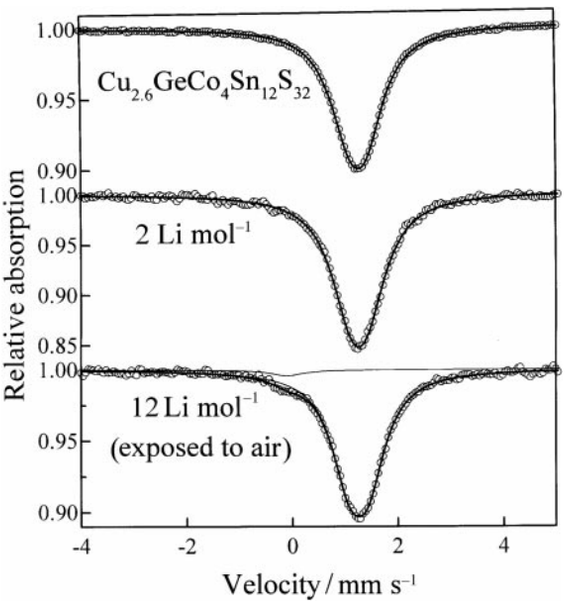

Fig. 6 Experimental and refined ^{119}Sn Mössbauer spectra of $Li_xCu_{2.6}GeCo_4Sn_{12}S_{32}$ at selected x values.

The ^{119}Sn Mössbauer spectrum of the $Cu_{2.6}GeCo_4Sn_{12}S_{32}$ powder is shown in Fig. 6, where only a single quadrupole-split signal with an isomer shift of 1.160(3) mm s^{-1} is present (Table 2), which is ascribable to Sn(IV). Additionally, the value of the quadrupolar splitting parameter (QS) indicates slight deviation from the cubic symmetry of the Sn^{IV} species. The origin of this may be due to three different effects:

(i) The nature of the equivalent sites occupied by tin atoms. These are 16d sites of the $Fd\bar{3}m$ space group, which have trigonal antiprismatic $\bar{3}m$ site symmetry. The trigonal distortion results from an x_S value slightly different from 1/4 (Table 1) and could explain the small but significant QS values.

(ii) The possible tetragonal distortion of the pseudo-octahedral sites induced by the Jahn–Teller effect which could affect Co^{II} ions in both high spin $t_{2g}^5e_g^2$ and especially low spin $t_{2g}^6e_g^1$ configurations. Owing to the random distribution of Sn^{IV} and Co^{II} in 16d sites, the distortion of the CoS_6 polyhedra may affect the equivalent SnS_6 sites. If true, this distortion is small, as it does not have a direct effect on the cubic unit cell. A dynamic Jahn–Teller distortion effect could also be invoked to explain the lack of detectable effects on the unit cell symmetry.

(iii) Last and less probable, the effect of second neighbors may induce a departure from spherical symmetry of the electric field affecting the tin nuclei. The different environments may

Table 2 Hyperfine parameters of the ^{119}Sn Mössbauer spectra of $Li_xCu_4GeCo_4Sn_{12}S_{32}$ and $Li_xCu_{2.6}GeCo_4Sn_{12}S_{32}$ for different x: isomer shift (IS), quadrupolar splitting (QS), line width (LW)

x	Assignment	IS/mm s^{-1}	QS/mm s^{-1}	LW/mm s^{-1}	Contribution (%)
$Li_xCu_4GeCo_4Sn_{12}S_{32}$					
0	Sn(IV)	1.173(6)	0.35(1)	1.10(1)	100
2	Sn(IV)	1.168(4)	0.34(1)	0.96(1)	100
12	Sn(IV)	1.174(7)	0.35(1)	0.95(1)	98
	Sn(II)	2.99(9)	0.27(1)	0.68(1)	2
16	SnO_2	−0.09(2)	—	0.88(7)	9
	Sn(IV)	1.191(6)	0.38(1)	0.87(2)	89
	Sn(II)	3.22(6)	0.56(7)	0.6(1)	2
$Li_xCu_{2.6}GeCo_4Sn_{12}S_{32}$					
0	Sn(IV)	1.160(3)	0.325(5)	0.873(5)	100
2	Sn(IV)	1.166(8)	0.32(1)	0.92(1)	100
12	SnO_2	−0.20(5)	—	0.72(2)	3
	Sn(IV)	1.163(2)	0.362(1)	0.83(1)	97

include Sn_6, Sn_5Co, Sn_4Co_2, … Co_6, taking into account the pseudo-octahedral neighbors, and Cu_6, Cu_5Ge, Cu_4Ge_2, … Ge_6, taking into account the tetrahedral neighbors. The weight of each of these possibilities could be derived from the distribution of ions and the stoichiometry ratios Cu/Ge = 4 and Sn/Co = 3. Nevertheless, as each one of these possibilities could induce a slightly different QS value, an unresolvable distribution in QS would result.

While the first interpretation is possible for any spinel-related solid, interpretation (ii) could offer interesting possibilities when comparing the pristine and chemically extracted materials. In this way, copper extraction could be accompanied by the oxidation of cobalt ions from Co^{II} to Co^{III}, thus preserving the electroneutrality of the solid, as found in related systems.[4] The most probable electronic configuration of Co^{II} and Co^{III} in the B sites (16d) of a spinel sulfide are low spin $t_{2g}^6e_g^1$ and $t_{2g}^6e_g^0$,[15] in which only the former is expected to show Jahn–Teller distortion. Thus, the pristine sample might show a slight tetragonal distortion, which is not expected in the copper-extracted sample. In consequence, the value of the quadrupolar splitting of the signal of the non-extracted sample should be slightly higher than for the extracted one. The observed data change by more than the sum of their standard deviations (Table 2) thus indicating that the Jahn–Teller effect may play a role. In order to confirm the effect of the Jahn–Teller distortion on the structure of the thiospinel, Rietveld refinement of the structural parameters of both samples was carried out by using the $I4_1/amd$ space group. This group was chosen on the basis of the structure of other spinels tetragonally distorted by the Jahn–Teller effect such as Mn_3O_4. In the new group, $a_T \approx 2^{-1/2}a$ and $c_T = a$, A ions are located in 4a sites (0,3/4,1/8), B ions in 8d (0,0,1/2) and sulfur in 16h (0,y,z) with $y \approx 0$ and $z \approx 1/4$. For $Cu_{2.6}GeCo_4Sn_{12}S_{32}$, no improvement in the goodness of fit was observed. By contrast, for $Cu_4GeCo_4Sn_{12}S_{32}$, a significant decrease of R_{Bragg} was obtained, from 4.82 to 3.40% (close to that obtained for the extracted sample, 3.21%). The c_T/a_T value, which can be obtained from the results in Table 1 was 1.4125(3), which is slightly lower than $2^{1/2}$. A similar tetragonal distortion has been described for the analogous compound $Cu_4GeFe_4Sn_{12}S_{32}$, also with $c/a < 2^{1/2}$, and having its origin in the low-spin configuration of Fe^{II}.[16]

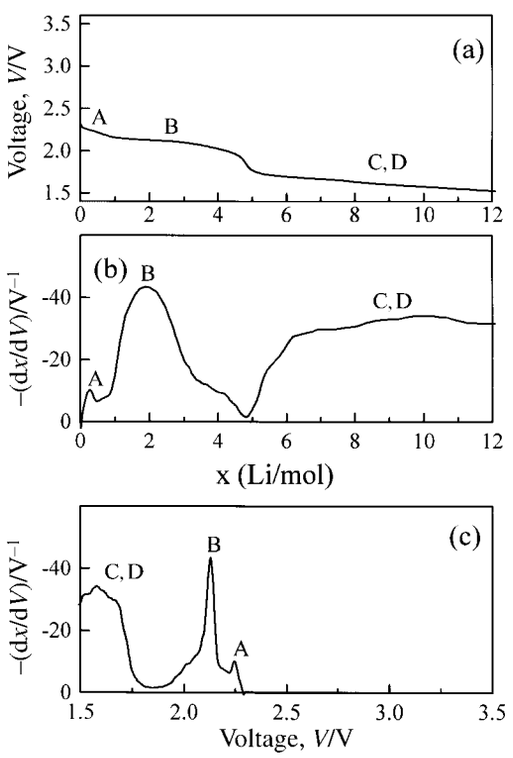

Fig. 7 Discharge curve of the cell $Li|LiClO_4–PC|Cu_{2.6}GeCo_4Sn_{12}S_{32}$: voltage V *vs.* x (a), $-dx/dV$ *vs.* x (b) and $-dx/dV$ *vs.* V (c).

Fig. 7 shows three representations of the discharge profile of $Cu_{2.6}GeCo_4Sn_{12}S_{32}$. The V *vs.* x (in $Li_xCu_{2.6}GeCo_4Sn_{12}S_{32}$) plot [Fig. 7(a)] reveals three well defined voltage steps A, B and C, D with plateaux located at *ca.* 2.24, 2.13 and 1.5–1.6 V. These steps are separated by a steep decrease in voltage at *ca.* 0.5 and 4.8 F mol^{-1}, leading to three separated reduction bands in the reciprocal derivative plot of $-dx/dV$ *vs.* x [Fig. 7(b)] and the corresponding peaks for the voltages in Fig. 7(c).

Ex situ XRD patterns of the lithium-inserted electrode pellets were obtained after interruption of the galvanostatic experiments at different depths of discharge. A selection of these patterns shown in Fig. 5 reveals that the spinel structure of the pristine chalcogenide is retained during electrochemical lithium insertion. Nevertheless, three main effects are observed: a loss of crystallinity evidenced by the enhanced line broadening, a significant increase in the relative intensity of the (111) reflection, and the occurrence of shoulders in the line profiles for $x \geqslant 8$. The increase in (111) line intensity is particularly evident from $x = 0$ to 4, but less marked changes are detected for larger depths of discharge. This result suggests a copper extraction process from 8a sites during the first step of the electrochemical lithium insertion. The Rietveld refined parameters from the X-ray diffraction patterns of the samples obtained at 4 and 6 F mol^{-1} are included in Table 1. It is of note that there is a decrease in the occupancy of Cu atoms in 8a sites, from *ca.* 2.6 at $x = 0$ to *ca.* 2.1 at $x = 4$ and $x = 6$.

The presence of shoulders in the XRD patterns for $x \geqslant 8$ is associated with larger error bars in the lattice parameter plot of Fig. 4; again for this two-phase region, the unit cell parameter corresponds to the more intense set of spinel reflections. As found for the pristine spinels, the insertion of lithium at cell potentials below 1.7 V involves the occupation of the 16c sites by the extra incoming lithium with possible spinel to rock-salt conversion. The fact that the two phase region is located for higher depth discharge in the chemically deintercalated solids agrees well with the previous extraction of copper, allowing a more extended insertion in tetrahedral sites before inducing the transformation to a rock-salt structure.

From the above results, the interpretation of the complex discharge curve in Fig. 7 should take into account the following effects.

(i) Filling of tetrahedral vacancies which were present in the pristine solid by incoming lithium ions. This process should account for 3 F mol^{-1} at a voltage of *ca.* 2.15 V with an origin similar to that suggested for peak B in Fig. 3.

(ii) Filling of tetrahedral vacancies created by prior chemical extraction of copper from 8a sites: *ca.* 1.4 F mol^{-1}, as revealed by the results in Table 1. This process should be accompanied by Co^{III}–Co^{II} reduction. A similar process was described in the related chemically extracted solid $CuCoSn_3S_8$ taking place at a cell potential of close to 2.2 V.[7] This value agrees well with the voltage of peak A in Fig. 7, although its exact value is difficult to assess owing to overlap with peak B. For ion-containing Cu-extracted solids, Fe^{III}–Fe^{II} reduction at a 2.6 V step potential electrochemical spectroscopy (SPES) peak was suggested.[5]

(iii) Simultaneous lithium insertion and copper reduction/extraction. This process can rationalize the lower site occupancy of 8a sites by copper after the first step of lithium insertion (*ca.* 0.5 F mol^{-1} according to Table 1). Indeed, a similar process was found to take place at potentials below 1.79 V *vs.* Li in $CuTiS_2$ spinels by Jacobsen *et al.*[17] Copper extraction occurring simultaneously with lithium insertion has also been reported in $Cu_2CoSn_3S_8$,[4] in which a voltage plateau at 1.6 V occurred simultaneously with the occurrence of Cu metal, as revealed by XRD. Thus, possible copper extraction at depths of discharge below peak C, D is difficult to interpret,

although its possible overlap with processes (i) and/or (ii) cannot be discarded.

The sum of contributions (i), (ii) and (iii) to the total cell capacity above 1.7 V (4.9 F mol^{-1}) fits well with the observed value of *ca.* 4.8 F mol^{-1} (Fig. 7).

Finally, a selection of the ^{119}Sn Mössbauer spectra recorded for lithium-inserted $Li_xCu_{2.6}GeCo_4Sn_{12}S_{32}$ samples at 2 F mol^{-1} intervals are shown in Fig. 6. The behaviour is similar to that described above for $Li_xCu_4GeCo_4Sn_{12}S_{32}$, where only one quadrupole-split signal is obtained for $x \leqslant 10$, which is characteristic of Sn^{IV} in a slightly distorted octahedral coordination. At $x = 12$, a second signal appears at *ca.* 0 mm s^{-1}. By comparison with the interpretation given to the spectrum of $Li_xCu_4GeCo_4Sn_{12}S_{32}$ at $x = 12$ and 16, the low intensity signal is attributable to the presence of SnO_2 derived from the oxidation of Sn^{II} by unavoidable contact with air. These results indicate that Sn^{IV}–Sn^{II} reduction takes place after extensive discharge, probably corresponding to step D, although the strong overlap observed between steps C and D does not allow the resolution of each effect.

Conclusion

A spinel sulfide was prepared as a polycrystalline material by direct synthesis. The solid shows a tetragonal distortion from the cubic $Fd\bar{3}m$ basic structure, as a result of the Jahn–Teller effect present for low spin Co^{II} ions. The lattice contains 3/8 of tetrahedral vacancies in 4a sites of the $I4_1/amd$ space group (8a in $Fd\bar{3}m$). Chemical extraction of copper from tetrahedral sites was achieved by using I_2–CH_3CN solutions to give $Cu_{2.6}GeCo_4Sn_{12}S_{32}$. Owing to the partial oxidation of Co^{II} to Co^{III}, the tetragonal distortion is negligible in the extracted solid. A Rietveld refinement in the $Fd\bar{3}m$ space group confirmed the occurrence of 4.4 tetrahedral vacancies in 8a sites.

The discharge curve using $Cu_4GeCo_4Sn_{12}S_{32}$ as an active cathode material in lithium anode cells reveals three well defined voltage steps denoted B, C and D, located at *ca.* 2.15, 1.67 V and < 1.65. The composition upper limit for step B agrees well with the number of Li atoms per unit cell formula required to fill the tetrahedral 8a sites of the cubic spinel structure. X-Ray diffraction patterns show that the spinel structure is preserved during the first steps of lithium insertion while for discharges with $x \geqslant 6$, a two-phase region occurs ascribable to the spinel to rock-salt structure transformation. ^{119}Sn Mössbauer spectroscopy allows step D to be attributed to Sn^{IV}–Sn^{II} reduction. When $Cu_{2.6}GeCo_4Sn_{12}S_{32}$ is used as the active cathode material, a new lithium insertion process appears in the first step of the discharge curve, centered at *ca.* 2.24 V. X-Ray diffraction patterns show that copper extraction takes place, increasing the total number of vacancies to 4.4 in 8a sites, close to the limit of step B in composition (*ca.* 4.8). The two phase-region occurs for deeper discharges in the chemically Cu-deinserted electrodes, ($x \geqslant 8$). The three different processes: vacancy filling, Co^{III}–Co^{II} and Cu^{I}–Cu^{0} reduction are not clearly resolved. ^{119}Sn Mössbauer spectroscopy shows that the Sn^{IV}–Sn^{II} reduction only takes place at large depths of discharge.

Acknowledgements

We are indebted to the Centre National de la Recherche Scientifique, France, for financial support (PICS N° 505). C.P.V. is also grateful to the European Community, Training and Mobility of Researchers program, contract number ERB-FMBI-CT98-3020.

References

1 J. C. Hunter, *J. Solid State Chem.*, 1981, **39**, 142.
2 M. L. Elidrissi Moubtassim, C. Bousquet, J. Olivier-Fourcade, J. C. Jumas and J. L. Tirado, *Chem. Mater.*, 1998, **10**, 968.
3 R. Schöllhorn and A. Payer, *Angew. Chem.*, 1985, **97**, 57.
4 P. Lavela, J. L. Tirado, J. Morales, J. Olivier-Fourcade and J. C. Jumas, *J. Mater. Chem.*, 1996, **6**, 41.
5 C. Bousquet, C. Pérez Vicente, A. Krämer, J. L. Tirado, J. Olivier-Fourcade and J. C. Jumas, *J. Mater. Chem.*, 1998, **8**, 1399.
6 N. Imanishi, K. Inoue, Y. Takeda and O. Yamamoto, *J. Power Sources*, 1993, **43/44**, 619.
7 M. A. Cochez, J. C. Jumas, P. Lavela, J. Morales, J. Olivier-Fourcade and J. L. Tirado, *J. Power Sources*, 1996, **62**, 101.
8 R. A. Young, A. Sakthivel, T. S. Moss and C. O. Paiva-Santos, *J. Appl. Crystallogr.*, 1995, **28**, 366.
9 W. Künding, *Nucl. Instrum. Methods*, 1969, **75**, 336.
10 M. M. Thackeray, W. I. F. David and J. B. Goodenough, *Mater. Res. Bull.*, 1982, **17**, 785.
11 C. J. Chen, M. Greenblatt and J. V. Waszczak, *Mater. Res. Bull.*, 1986, **21**, 609.
12 M. M. Thackeray, *J. Electrochem. Soc.*, 1995, **142**, 2558.
13 A. C. W. James, B. Ellis and J. B. Goodenough, *Solid State Ionics*, 1988, **27**, 45.
14 D. O'Hare, W. Laegermann, D. L. Williamson, F. S. Ohuchi and A. Parkinson, *Inorg. Chem.*, 1988, **27**, 1537.
15 J. B. Goodenough, *J. Phys. Chem. Solids*, 1969, **30**, 261.
16 J. C. Jumas, E. Philippot and M. Maurin, *Acta Crystallogr., Sect. B*, 1979, **35**, 2195.
17 T. Jacobsen, B. Zachau-Christiansen, K. West and S. Atlung, *Electrochim. Acta*, 1989, **34**, 1473.

Paper 9/02630D